

# Supervised NDVI Composite Thresholding for Arid Region Vegetation Mapping

## Ragab Khalil

Civil Engineering Department, Faculty of Engineering, Assiut University, Egypt | Department of Civil Engineering, College of Engineering and Information Technology, Onaizah Colleges, Saudi Arabia  
ragab2khalil@gmail.com

## Mohammad Shahiq Khan

Department of Civil Engineering, College of Engineering and Information Technology, Onaizah Colleges, Saudi Arabia  
shahiqitr@gmail.com

## Yassin Hasan

Department of Electrical Engineering, College of Engineering and Information Technology, Onaizah Colleges, Saudi Arabia  
yhassan@oc.edu.sa

## Nacer Nacer

Department of Civil Engineering, College of Engineering and Information Technology, Onaizah Colleges, Saudi Arabia  
n.nacer@oc.edu.sa

## Sheroz Khan

Department of Electrical Engineering, College of Engineering and Information Technology, Onaizah Colleges, Saudi Arabia  
cnar32.sheroz@gmail.com (corresponding author)

Received: 6 March 2024 | Revised: 19 March 2024 | Accepted: 21 March 2024

Licensed under a CC-BY 4.0 license | Copyright (c) by the authors | DOI: <https://doi.org/10.48084/etasr.7202>

## ABSTRACT

Temporal-vegetation mapping bearing temporal-related features is important because it helps to understand the global climate changes that drive resource management and habitat conservation. This paper presents a Supervised Normalized Difference Vegetation Index (SNDVI) approach for mapping the vegetation cover in arid environment regions. The NDVI is used to extract features to classify land as a vegetation cover, water body, or bare soil. Through the use of Normalized Difference Vegetation Index (NDVI), regions can be categorized as dry or sandy, based on the soil reflectance values. NDVI is the most commonly deployed index for accurate vegetation cover estimates. The NDVI values lie in a range from -1 to +1, depending on the environmental region and vegetation conditions. It is difficult to assign a specific threshold value to distinguish between vegetation and non-vegetation for all the eco-regions under a specific landscape and ecological conditions. The proposed approach is based on the quantitative verification of the samples as well as the supervised classification method followed to categorize the images. The SNDVI approach has been applied to three different locations in three different seasons in arid ecoregions to extract features for vegetation mapping. The results disclose that SNDVI is a very reliable parameter in extracting true vegetation cover in arid regions. An accuracy evaluation matrix has been performed for each case study and the overall obtained accuracy value ranged from 82% to 100%, depending on the season of the area under investigation. The utility of the proposed method is determined by bench-marking the results with those of the techniques recently utilized by contemporary researchers.

*Keywords-vegetation indices; crop land mapping; remote sensing*

## I. INTRODUCTION

Natural resources are managed and preserved through estimating the vegetation cover maps of the target regions because vegetation plays a critical role in influencing climate changes by providing the primary habitat for all living things. Cover maps also help in the policy-making of ecosystem management. They offer basic information to estimate the vegetation cover over a continuous period of time to identify and describe natural and artificially maintained environments in detail. It is necessary, therefore, to find out the present status of the vegetation conditions in order to plan vegetation conservation strategies or other similar vegetation-related restoration programs properly at a national scale level [1, 2]. Mapping has been used to identify rice fields [3], for the understanding and precise monitoring of the land cover in order to manage and improve crop production [4]. Alternatively, spatial resolution has been deployed for visual illumination [5]. Remote sensing technology provides practical and budgetary ways to explore the vegetation cover compared to traditional methods, especially in vastly dispersed areas. The multispectral bands of satellite images allow the extraction of valuable information related to the landscape, including the vegetation cover. Vegetation can be identified by employing satellite images of all the visible features of a land area based on its identifiable spectral characteristics. The development of remote sensing has led to the extraction of several spectral indices that are utilized as the most effective means of measuring the specific attributes of land to understand the extent of vegetation cover [6]. The most commonly used index due to its general usefulness is the Normalized Difference Vegetation Index (NDVI). The latter is put into service for estimating the vegetation cover across diverse domains of interest [7]. The NDVI is calculated from multispectral information as a normal ratio of the red to near-infrared frequency spectrums [8]. It is the most widely exploited spectral Vegetation Index (VI) by ecologists and agriculturalists today [9]. The NDVI is a productivity parameter and has been used to measure and monitor the environmental conditions in terms of yield estimation to understand the fertility of a region [10–12], to help in precision farming [13], to mitigate land degradation [14], in dry land studies [15–18], and in the estimation of the vegetation cover acreage [19]. The NDVI is calculated as a simple numerical value to assess from afar the area or object under study and to measure the livable green vegetation [20, 21]. The NDVI is computed by:

$$\text{NDVI} = (\text{NIR} - \text{Red}) / (\text{NIR} + \text{Red}) \quad (1)$$

where Red is the visible red reflectance, and NIR the near-infrared reflectance.

The values of NDVI extend from -1 to +1 to provide information on spatiotemporal changes in vegetation distribution, and to offer further knowledge about the habitats and the ecological effects of disasters. Higher NDVI values mean higher green intensity and vice versa. The NDVI prediction gives a close to accurate analysis of the land cover characteristics [22]. This paper does not rely on deploying fixed threshold values to describe terrain features. Instead, most of this work has made use of study-specific criteria. While

some researchers divide the NDVI index into different categories of regions, very low NDVI values of 0.1 and below correspond to arid, rocky, sandy, and snowy regions. Medium values of 0.2 to 0.3 show shrubs and grassy lands, whereas higher values in the range of 0.6 to 0.8 represent temperate and tropical rain-forests [23]. Barren soils are symbolized by NDVI values close to 0 and water bodies are denoted by NDVI values in the negative range [24]. Other researchers divide the range where negative values refer to areas with water, swampy surfaces, man-made structures, rocks, clouds, and snow, whereas bare land usually gives values that fall within 0.1 to 0.2. Vegetation, however, always has positive values between 0.2 and 1. For dense and healthy vegetation, the values are above 0.5, whereas for sparse vegetation the values range from 0.2 to 0.5 [25]. Other researchers reported that NDVI values belong to the general 0.2 to 0.4 range for areas of sparse vegetation and 0.4 to 0.6 for temperate vegetation, whereas values higher than 0.6 indicate the highest possible green intensity. These fuzzy thresholds lead to differences in the estimation of the area of the land-cover features as suggested in [17, 26]. This research aims to develop a cost-effective and reliable approach to extract vegetation and non-vegetation land cover and to produce accurate vegetation mapping in arid environment zones through the proposed Supervised NDVI (SNDVI) indexing technique. The main contributions of the paper are summarized as:

- The results in this paper do not rely on employing fixed threshold values that lead to having diversely ranging index values for varying vegetation covers.
- The proposed SNDVI technique extracts features that represent the vegetation and non-vegetation cover more accurately than other contemporary techniques, as listed in Table III.

## II. STUDY AREA

The area under examination lies in the north-western side of the Kingdom of Saudi Arabia, between the latitudes 26° N and 27° N and with longitudes 37° E and 38° E, within the Madinah region as observed in Figure 1. Three locations of 100 km<sup>2</sup> are selected, each with sparse natural vegetation and each representing different backgrounds and varying amounts of vegetation. The first location contains sparse natural vegetation and a collection of valleys of fine gray sand and gray rocks in the western part and shiny sands and yellow rocks in the eastern part. The second location entails only sparse natural vegetation and bright white to yellow rocks and sandy structure formations next to rocks of different shades of gray areas. The third location involves a strip of farms in the western and northern part with sparse natural vegetation against a bright yellow background of sand and rocks. The study area represents an arid environment zone with a maximum monthly precipitation of 22 mm and a maximum temperature of 40 °C [27].

## III. DATA COLLECTION

Three Sentinel-2 level 1C satellite images were downloaded from the Earth Explorer website. The image acquisition dates are in January, April, and August and are chosen to cover

minimum, moderate, and maximum temperatures and precipitation rates in the study area, which affect the vegetation in each image. Sentinel images are free and are generally used to estimate vegetation. The pseudo color combinations from Band 3 (B3, green), Band 4 (B4, Red), and Band 8 (B8, NIR) were performed (Figure 1) for visual interpretation of the images. Band 4 (Red) and Band 8 (NIR) are extracted for each study site to separately calculate the NDVI. The climate data for temperature and precipitation were obtained from the Climate Change Knowledge Portal [27].

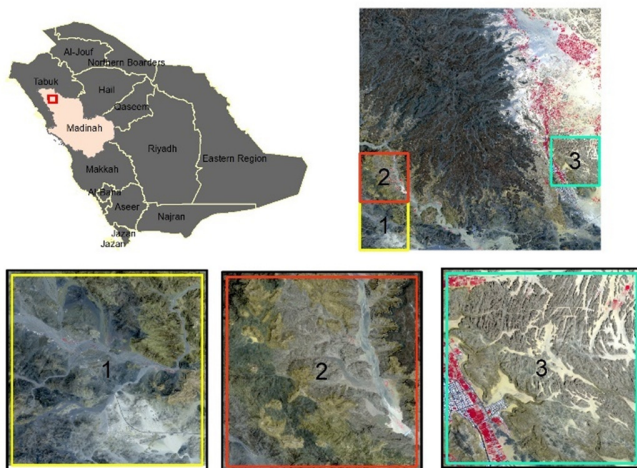


Fig. 1. Location map of the study area.

#### IV. THE PROPOSED APPROACH

The main idea of the proposed approach is to extract the NDVI values representing vegetation and non-vegetation related traits from a set of control or training points as composite site values, which are to be used as thresholds for vegetation mapping. The steps of the suggested approach are manifested in Figure 2. The first step is to produce a false color image for the visual interpretation of the satellite location image. The second step is to calculate the NDVI in order to compute the Vegetation Condition Index (VCI) accordingly. The third step relates to the generation of sample points for vegetation and non-vegetation land-cover traits. The fourth step is to utilize training points on both vegetation and non-vegetation features to extract the VCI values. The fifth step is to generate vegetation maps employing the extracted VCI values. The final step is to assess the accuracy of the generated maps.

##### A. Band Combination

A false color image is created using the green, red and infrared frequency spectra (B3, B4, B8 in Sentinel 2) to easily distinguish the vegetation from the non-vegetation features. The latter also helps in choosing the location of the training and assessment points. Three false color images for January, April, and August are produced for the three study zones.

##### B. Vegetation Condition Index (VCI)

The minimum and maximum values of NDVI vary from site to site. In this study, the scaled NDVI values are calculated.

These scaled values range from 0 to 1 and are known as vegetation coverage index [5], green vegetation fraction [28], proportion of vegetation [29], or VCI [30], which can be derived by:

$$VCI = (NDVI - NDVI_{min}) / (NDVI_{max} - NDVI_{min}) \quad (2)$$

where  $NDVI_{min}$  and  $NDVI_{max}$  are the Minimum and Maximum values of the NDVI, respectively.

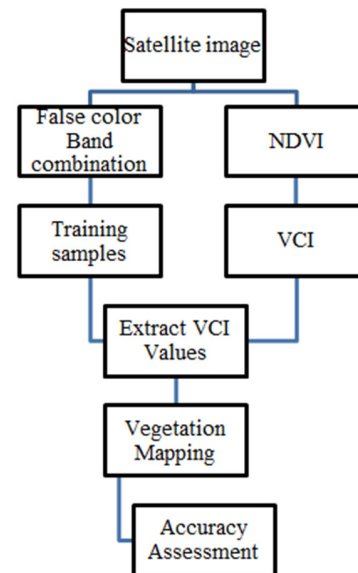


Fig. 2. Flowchart of the proposed approach.

Deploying the Sentinel 2 image, the NDVI is calculated for each pixel using Band-4 and Band-8. The minimum and maximum values of NDVI for the study zones are subsequently determined. Depending on (2), a vegetation cover map of the area under exploration is generated and extracted utilizing 80 training points, 40 points on vegetation and another 40 on non-vegetation features as displayed in Figure 3.

##### C. Vegetation Maps

After extracting the VCI values, the vegetation maps are created for the three study zones in three different seasons with four proposed threshold values of the VCI. These thresholds will be numbered as threshold 1 to threshold 4 where:

- Threshold 1 is the minimum VCI value of vegetation features.
- Threshold 2 is the maximum VCI value of non-vegetation features.
- Threshold 3 is the average of the VCI values of non-vegetation features.
- Threshold 4 is the average of the minimum VCI value of vegetation and the maximum VCI value of non-vegetation features.

Each study zone contains four maps for each season, which means 12 maps for each zone. This makes a total of 36 combinations for the three study zones.

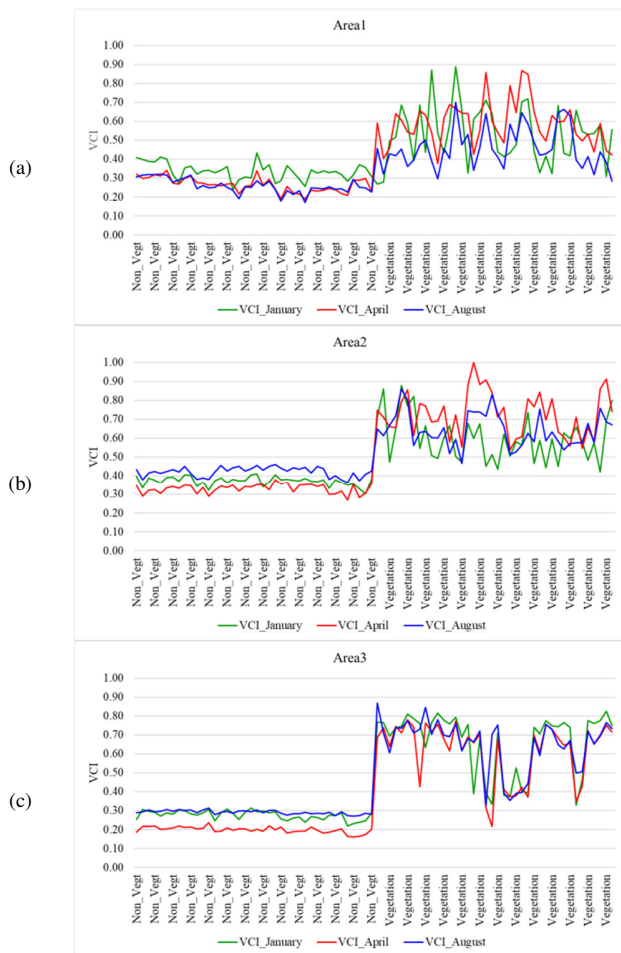


Fig. 3. Extracted values of VCI.

D. Accuracy Assessment

The accuracy assessment of the generated vegetation maps can be described as the procedure of comparing the generated map with the geographical data assumed to be correct. Usually, a set of reference pixels is implemented where the actual data on the generated map are known. The relationship between these two comparative pieces of information is commonly summarized in an error matrix. In this study, the number of the reference points used to assess the accuracy of the resulting vegetation maps is 80, 40 on the vegetation and 40 on non-vegetation features. The overall accuracy and Kappa (statistical discrepancy measure) coefficient are computed utilizing the error matrix data.

V. RESULTS AND DISCUSSION

Data samples from Zones-1, 2, and 3, and the results are shown in Figures 4, 5, and 6, respectively. The false color composite from Sentinel-2 is portrayed in Figure (a), where vegetation features appear in the shade of red, whereas Figures (b)-(e) exhibit the results derived from applying the four proposed thresholds. The estimated vegetated areas are demonstrated in green color whereas the non-vegetated areas are shown without color. From Figure 4, it can be noticed that the vegetation map generated using Threshold 2 is closest to

the actual vegetation areas depicted in the satellite image. The maps in Figures 4-6 were produced employing the VCI raster layer. Reclassification is the procedure of setting up in a raster dataset of one or more values to specify the resulting outcome values. The reclassification tool can be used in the Spatial Analyst extension in ArcMap. The normal work flow for users in ArcMap has been to begin with the raster layer code rendering varying algorithms meant for classification. After displaying the layer and being complied with the classification reassigned values, the Classify option can be utilized once the Reclassify tool is opened to reproduce the choice classification and class intervals. In this study, the mapping intervals are the suggested VCI thresholds using the described before values extracted for sampling data.

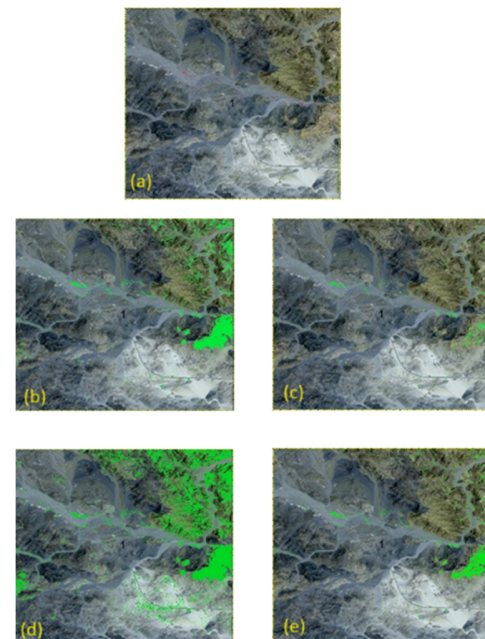


Fig. 4. Vegetation maps of Zone 1 in August using: (a) Sentinel-2 false color over the area of interest, (b) Threshold 1, (c) Threshold 2, (d) Threshold 3, (e) Threshold 4.

Table I illustrates the error matrices for the four thresholds of Zone 1 in August and other derived statistical parameters. It can be observed that the best overall accuracy of 96.25% was obtained employing Threshold 2 while the Kappa coefficient was 92.5. The second-best overall accuracy of 88.75% was acquired deploying Threshold 4 with a Kappa coefficient of 77.50. The third-best overall accuracy of 85% was attained using Threshold 1 with a Kappa coefficient equal to 70.00. The minimum overall accuracy of 80.00% was reached engaging Threshold 3 with a Kappa coefficient equal to 60.00. Table II displays the accuracy and Kappa coefficient of the four threshold methods in the three study zones for the three environmental seasons. It can be noticed from the Tables and with reference to Figures 4-6 that the best results were obtained when using Threshold 2, since they are higher than or equal to those of other thresholds in all seasons for all study zones. The results of implementing Threshold 2 are very close to those of Threshold 1 and Threshold 4 for Zone 2 in April and August.

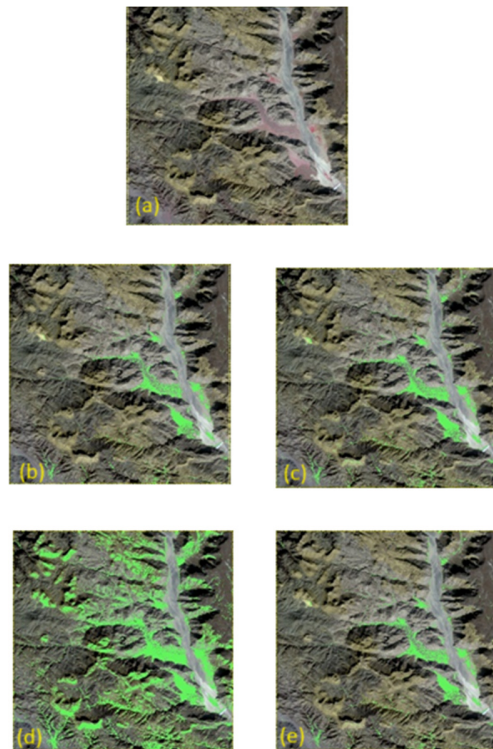


Fig. 5. Vegetation maps of Zone 2 in August using: (a) Sentinel-2 false color over the area of interest, (b) Threshold 1, (c) Threshold 2, (d) Threshold 3, (e) Threshold 4.

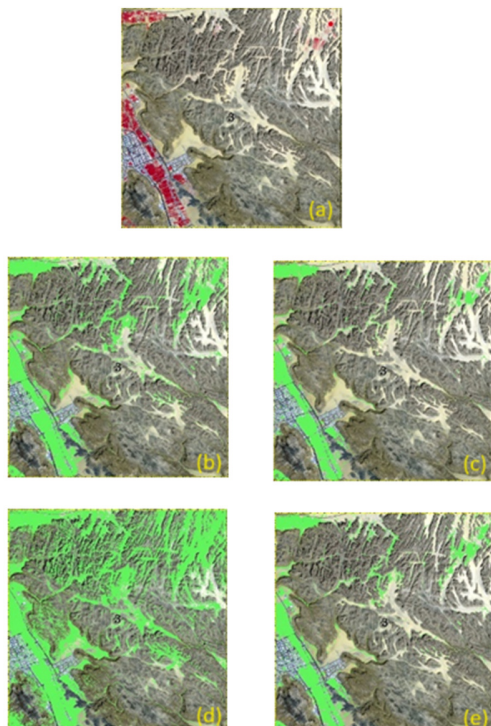


Fig. 6. Vegetation maps of Zone 3 in August using: (a) Sentinel-2 false color over the area of interest, (b) Threshold 1, (c) Threshold 2, (d) Threshold 3, (e) Threshold 4.

The results disclose that Threshold 2 is recommended to be used in the generation of vegetation maps during all seasons for all study areas.

### VI. COMPARISON AND CROSS VALIDATION

For cross validation, the vegetation maps were generated implementing the procedure and thresholds reported in [31], based on the study in Australia in which fixed threshold values were used. Results manifesting arid zones are reported in [32] by classifying the target area into non-vegetation and vegetation, utilizing NDVI values less than 0.19 to extract features related to the non-vegetation district. The features related to the vegetation region such as green cover, shrubs, and trees are extracted by employing NDVI values higher than 0.19. Following the same procedure with fixed threshold values, the results of Figure 7 are obtained on the Sentinel-2 pictures. These findings can be compared with the results portrayed in Figures 4-6, which were acquired by the proposed procedure. The former results are outstandingly clearer when compared to the latter.

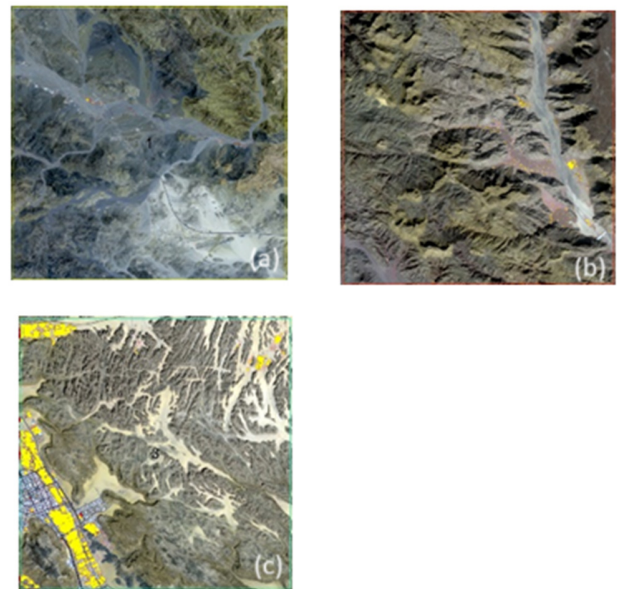


Fig. 7. Vegetation maps using the threshold of [31]: (a) Zone-1, (b) Zone-2, (c) Zone-3.

Comparing Figures 4-6 to Figure 7, it is clear that using fixed NDVI threshold values leads to generating vegetation maps that are not as outstandingly clear as the ones produced by the proposed SNDVI approach for the mapping of arid environment zones. Much of the natural vegetation areas appear to be lost due to the employment of fixed NDVI threshold values. The accuracy of vegetation maps in Figure 7 produced by the procedure of [31] is evaluated against the maps of Figure 4-6. The accuracy matrices are listed in Table III.

It is evident from Table III that the results of the proposed approach in extracting the vegetation cover are more accurate than those of the fixed threshold value procedure. The overall accuracy for Zone 3 in Table III is high due to the agriculture

plantations that represent the main green cover in the study area. The natural vegetation appears to be lost in the three study areas. The overall accuracies for Zone 1, Zone 2, and Zone 3

using the procedure of [31] are 90, 75, and 40%, respectively compared to the obtained 96.25, 98.75, and 100.00%, correspondingly from the proposed procedure.

TABLE I. ACCURACY ASSESSMENT OF THRESHOLD (A) 1, (B) 2, (C) 3, AND (D) 4, ON ZONE 1 IN AUGUST

<b>(A) Threshold 1 (August)</b>					
<b>Predicted</b>					
Land cover	Non-Vegetation	Vegetation	Total Row	P accuracy	Omission Error
Reference Non-Vegetation	29	11	40	72.50	27.50
Reference Vegetation	1	39	40	97.50	2.50
<b>Total Column</b>	30	50	80		
<b>U Accuracy</b>	96.67	78.00		Overall accuracy	<b>85.00</b>
<b>Commission Error</b>	3.33	22.00		Kappa Coefficient	<b>70.00</b>

<b>(B) Threshold 2 (August)</b>					
<b>Predicted</b>					
Land cover	Non-Vegetation	Vegetation	Total Row	P accuracy	Omission Error
Reference Non-Vegetation	40	0	40	100.00	0.00
Reference Vegetation	3	37	40	92.50	7.50
<b>Total Column</b>	43	37	80		
<b>U Accuracy</b>	93.02	100.00		Overall accuracy	<b>96.25</b>
<b>Commission Error</b>	6.98	0.00		Kappa Coefficient	<b>92.50</b>

<b>(C) Threshold 3 (August)</b>					
<b>Predicted</b>					
Land cover	Non-Vegetation	Vegetation	Total Row	P accuracy	Omission Error
Reference Non-Vegetation	24	16	40	60.00	40.00
Reference Vegetation	0	40	40	100.00	0.00
<b>Total Column</b>	24	56	80		
<b>U Accuracy</b>	100.00	71.43		Overall accuracy	<b>80.00</b>
<b>Commission Error</b>	0.00	28.57		Kappa Coefficient	<b>60.00</b>

<b>(D) Threshold 4 (August)</b>					
<b>Predicted</b>					
Land cover	Non-Vegetation	Vegetation	Total Row	P accuracy	Omission Error
Reference Non-Vegetation	33	7	40	82.50	17.50
Reference Vegetation	2	38	40	95.00	5.00
<b>Total Column</b>	35	45	80		
<b>U Accuracy</b>	94.29	84.44		Overall accuracy	<b>88.75</b>
<b>Commission Error</b>	5.71	15.56		Kappa Coefficient	<b>77.50</b>

TABLE II. ACCURACY ASSESSMENT OF (A) ZONE 1, (B) ZONE 2, AND (C) ZONE 3 IN JANUARY, APRIL, AND AUGUST.

<b>(A) Zone 1</b>	<b>January</b>		<b>April</b>		<b>August</b>	
Method	Overall Accuracy	Kappa	Overall Accuracy	Kappa	Overall Accuracy	Kappa
Threshold 1	52.50	5.00	98.75	97.50	85.00	70.00
Threshold 2	82.50	65.00	100.00	100.00	96.25	92.50
Threshold 3	67.50	35.00	75.00	50.00	80.00	60.00
Threshold 4	75.00	50.00	100.00	100.00	88.75	77.50

<b>(B) Zone 2</b>	<b>January</b>		<b>April</b>		<b>August</b>	
Method	Overall Accuracy	Kappa	Overall Accuracy	Kappa	Overall Accuracy	Kappa
Threshold 1	98.75	97.50	100.00	100.00	98.75	97.50
Threshold 2	100.00	100.00	98.73	97.47	98.75	97.50
Threshold 3	71.25	42.50	70.00	40.00	71.25	42.50
Threshold 4	100.00	100.00	100.00	100.00	100.00	100.00

<b>(C) Zone 3</b>	<b>January</b>		<b>April</b>		<b>August</b>	
Method	Overall Accuracy	Kappa	Overall Accuracy	Kappa	Overall Accuracy	Kappa
Threshold 1	98.75	97.50	92.50	85.00	100.00	100.00
Threshold 2	98.75	97.50	97.50	95.00	100.00	100.00
Threshold 3	71.25	42.50	73.75	47.50	76.25	52.50
Threshold 4	100.00	100.00	97.50	95.00	100.00	100.00

TABLE III. ACCURACY ASSESSMENT OF VEGETATION MAPS GENERATED USING THRESHOLDS OF [31] ZONE (A) 1, (B) 2, AND (C) 3

		Predicted					
(A) Zone 1	Land cover	Non-Vegetation	Vegetation	Total Row	P accuracy	Omission Error	
Reference	Non-Vegetation	32	8	40	80.00	20.00	
	Vegetation	40	0	40	0.00	100.00	
	Total Column	72	8	80			
	U Accuracy	44.44	0.00		Overall accuracy	40.00	
	Commission Error	55.56	100.00		Kappa Coefficient	-20.00	

		Predicted					
(B) Zone 2	Land cover	Non-Vegetation	Vegetation	Total Row	P accuracy	Omission Error	
Reference	Non-Vegetation	40	0	40	100.00	0.00	
	Vegetation	20	20	40	50.00	50.00	
	Total Column	60	20	80			
	U Accuracy	66.67	100.00		Overall accuracy	75.00	
	Commission Error	33.33	0.00		Kappa Coefficient	50.00	

		Predicted					
(C) Zone 3	Land cover	Non-Vegetation	Vegetation	Total Row	P accuracy	Omission Error	
Reference	Non-Vegetation	39	1	40	97.50	2.50	
	Vegetation	7	33	40	82.50	17.50	
	Total Column	46	34	80			
	U Accuracy	84.78	97.06		Overall accuracy	90.00	
	Commission Error	15.22	2.94		Kappa Coefficient	80.00	

## VII. CONCLUSION

In this study, vegetation cover maps were generated by utilizing the proposed Supervised NDVI approach (SNDVI) in three arid regions located in northwestern Saudi Arabia. This approach solves the problem of using fixed of constant threshold values when estimating the vegetation cover from satellite images. The proposed SNDVI approach relies on agile threshold values depending on the site and vegetation cover to generate vegetation maps from satellite images. The research investigates four methods of extracting the threshold values according to the scaled NDVI Vegetation Condition Index (VCI) values. In these four methods, the threshold values were calculated as: Threshold 1 as the minimum VCI value of vegetation features, Threshold 2 as the maximum VCI value of non-vegetation features, Threshold 3 as the average of the VCI values of non-vegetation features, and Threshold 4 as the average of the minimum VCI value of vegetation and maximum VCI value of non-vegetation features. These threshold values were applied to the three study zones with different vegetation densities in three environmental seasons. After vegetation mappings were developed, the accuracy was estimated. The scaled NDVI values were extracted using 40 testing points on vegetation features and 40 points on non-vegetation features. It has been concluded that applying Threshold 2 gives the best overall accuracy and generates the more precise vegetation maps. Among the proposed thresholds, as listed in Table II, Threshold 2 values exhibit the best performance for all study zones and seasons. The technique of obtaining a threshold value is the most simple and accurate thresholding technique for generating vegetation cover maps. From the cross validation process it can be concluded that the proposed SNDVI approach is simple in implementation and offers more accurate results than the ones acquired when using a fixed value, showing accuracy of 96.25% (compared to 90%), 98.75% (compared to 75%) and 100% (compared to 40%).

## DATA AVAILABILITY STATEMENT

The satellite images used in this research are taken from <https://earthexplorer.usgs.gov/>

## REFERENCES

- [1] Y. Xie, Z. Sha, and M. Yu, "Remote sensing imagery in vegetation mapping: a review," *Journal of Plant Ecology*, vol. 1, no. 1, pp. 9–23, Mar. 2008, <https://doi.org/10.1093/jpe/rtm005>.
- [2] C. He, Q. Zhang, Y. Li, X. Li, and P. Shi, "Zoning grassland protection area using remote sensing and cellular automata modeling—A case study in Xilingol steppe grassland in northern China," *Journal of Arid Environments*, vol. 63, no. 4, pp. 814–826, Dec. 2005, <https://doi.org/10.1016/j.jaridenv.2005.03.028>.
- [3] P. S. Nagendram, P. Satyanarayana, and P. R. Teja, "Mapping Paddy Cropland in Guntur District using Machine Learning and Google Earth Engine utilizing Images from Sentinel-1 and Sentinel-2," *Engineering, Technology & Applied Science Research*, vol. 13, no. 6, pp. 12427–12432, Dec. 2023, <https://doi.org/10.48084/etasr.6460>.
- [4] M. K. Villareal and A. F. Tongco, "Remote Sensing Techniques for Classification and Mapping of Sugarcane Growth," *Engineering, Technology & Applied Science Research*, vol. 10, no. 4, pp. 6041–6046, Aug. 2020, <https://doi.org/10.48084/etasr.3694>.
- [5] H. Tahir and A. H. M. Din, "The Potential of Landsat 8 OLI Images in Coastline Identification: The Case Study of Basra, Iraq," *Engineering, Technology & Applied Science Research*, vol. 14, no. 1, pp. 13041–13046, Feb. 2024, <https://doi.org/10.48084/etasr.6580>.
- [6] C. Eisfelder, C. Kuenzer, and S. Dech, "Derivation of biomass information for semi-arid areas using remote-sensing data," *International Journal of Remote Sensing*, vol. 33, no. 9, pp. 2937–2984, May 2012, <https://doi.org/10.1080/01431161.2011.620034>.
- [7] D. Moravec, J. Komarek, S. Lopez-Cuervo Medina, and I. Molina, "Effect of Atmospheric Corrections on NDVI: Intercomparability of Landsat 8, Sentinel-2, and UAV Sensors," *Remote Sensing*, vol. 13, no. 18, Jan. 2021, Art. no. 3550, <https://doi.org/10.3390/rs13183550>.
- [8] A. Karnieli *et al.*, "Use of NDVI and Land Surface Temperature for Drought Assessment: Merits and Limitations," *Journal of Climate*, vol. 23, no. 3, pp. 618–633, Feb. 2010, <https://doi.org/10.1175/2009JCLI2900.1>.
- [9] A. L. Yagci, L. Di, and M. Deng, "The influence of land cover-related changes on the NDVI-based satellite agricultural drought indices," in *IEEE Geoscience and Remote Sensing Symposium*, Quebec City, QC,

- Canada, Jul. 2014, pp. 2054–2057, <https://doi.org/10.1109/IGARSS.2014.6946868>.
- [10] S. S. Panda, D. P. Ames, and S. Panigrahi, "Application of Vegetation Indices for Agricultural Crop Yield Prediction Using Neural Network Techniques," *Remote Sensing*, vol. 2, no. 3, pp. 673–696, Mar. 2010, <https://doi.org/10.3390/rs2030673>.
- [11] M. S. Mkhabela, P. Bullock, S. Raj, S. Wang, and Y. Yang, "Crop yield forecasting on the Canadian Prairies using MODIS NDVI data," *Agricultural and Forest Meteorology*, vol. 151, no. 3, pp. 385–393, Mar. 2011, <https://doi.org/10.1016/j.agrformet.2010.11.012>.
- [12] J. White, A. A. Berg, C. Champagne, Y. Zhang, A. Chipanshi, and B. Daneshfar, "Improving crop yield forecasts with satellite-based soil moisture estimates: An example for township level canola yield forecasts over the Canadian Prairies," *International Journal of Applied Earth Observation and Geoinformation*, vol. 89, Jul. 2020, Art. no. 102092, <https://doi.org/10.1016/j.jag.2020.102092>.
- [13] T. L. Nordblom, T. R. Hutchings, S. S. Godfrey, and C. R. Scheffe, "Precision variable rate nitrogen for dryland farming on waterlogging Riverine Plains of Southeast Australia?," *Agricultural Systems*, vol. 186, Jan. 2021, Art. no. 102962, <https://doi.org/10.1016/j.agsy.2020.102962>.
- [14] R. M. Fokeng and Z. N. Fogwe, "Landsat NDVI-based vegetation degradation dynamics and its response to rainfall variability and anthropogenic stressors in Southern Bui Plateau, Cameroon," *Geosystems and Geoenvironment*, vol. 1, no. 3, Aug. 2022, Art. no. 100075, <https://doi.org/10.1016/j.geogeo.2022.100075>.
- [15] M. Aboelghar, S. Arafat, A. Saleh, S. Naeem, M. Shirbeny, and A. Belal, "Retrieving leaf area index from SPOT4 satellite data," *The Egyptian Journal of Remote Sensing and Space Science*, vol. 13, no. 2, pp. 121–127, Dec. 2010, <https://doi.org/10.1016/j.ejrs.2010.06.001>.
- [16] D. Dutta, A. Kundu, and N. R. Patel, "Predicting agricultural drought in eastern Rajasthan of India using NDVI and standardized precipitation index," *Geocarto International*, vol. 28, no. 3, pp. 192–209, Jun. 2013, <https://doi.org/10.1080/10106049.2012.679975>.
- [17] S. Mondal, C. Jeganathan, N. K. Sinha, H. Rajan, T. Roy, and P. Kumar, "Extracting seasonal cropping patterns using multi-temporal vegetation indices from IRS LISS-III data in Muzaffarpur District of Bihar, India," *The Egyptian Journal of Remote Sensing and Space Science*, vol. 17, no. 2, pp. 123–134, Dec. 2014, <https://doi.org/10.1016/j.ejrs.2014.09.002>.
- [18] M. Roznik, M. Boyd, and L. Porth, "Improving crop yield estimation by applying higher resolution satellite NDVI imagery and high-resolution cropland masks," *Remote Sensing Applications: Society and Environment*, vol. 25, Jan. 2022, Art. no. 100693, <https://doi.org/10.1016/j.rsase.2022.100693>.
- [19] P. Fabijanczyk and J. Zawadzki, "Spatial correlations of NDVI and MSAVI2 indices of green and forested areas of urban agglomeration, case study Warsaw, Poland," *Remote Sensing Applications: Society and Environment*, vol. 26, Apr. 2022, Art. no. 100721, <https://doi.org/10.1016/j.rsase.2022.100721>.
- [20] H. Demirel, C. Ozcinar, and G. Anbarjafari, "Satellite Image Contrast Enhancement Using Discrete Wavelet Transform and Singular Value Decomposition," *IEEE Geoscience and Remote Sensing Letters*, vol. 7, no. 2, pp. 333–337, Apr. 2010, <https://doi.org/10.1109/LGRS.2009.2034873>.
- [21] X. Zhang, Y. Hu, D. Zhuang, Y. Qi, and X. Ma, "NDVI spatial pattern and its differentiation on the Mongolian Plateau," *Journal of Geographical Sciences*, vol. 19, no. 4, pp. 403–415, Aug. 2009, <https://doi.org/10.1007/s11442-009-0403-7>.
- [22] M. S. Omar and H. Kawamukai, "Prediction of NDVI using the Holt-Winters model in high and low vegetation regions: A case study of East Africa," *Scientific African*, vol. 14, Nov. 2021, Art. no. e01020, <https://doi.org/10.1016/j.sciaf.2021.e01020>.
- [23] D. Dutta, A. Kundu, N. R. Patel, S. K. Saha, and A. R. Siddiqui, "Assessment of agricultural drought in Rajasthan (India) using remote sensing derived Vegetation Condition Index (VCI) and Standardized Precipitation Index (SPI)," *The Egyptian Journal of Remote Sensing and Space Science*, vol. 18, no. 1, pp. 53–63, Jun. 2015, <https://doi.org/10.1016/j.ejrs.2015.03.006>.
- [24] R. Chouhan and N. Rao, "Vegetation Detection in Multispectral Remote Sensing Images: Protective Role-Analysis of Vegetation in 2004 Indian Ocean Tsunami," in *Gi4DM 2011: GeoInformation for disaster management*, 2011.
- [25] A. Zaitunah, Samsuri, and F. Sahara, "Mapping and assessment of vegetation cover change and species variation in Medan, North Sumatra," *Heliyon*, vol. 7, no. 7, Jul. 2021, Art. no. e07637, <https://doi.org/10.1016/j.heliyon.2021.e07637>.
- [26] A. Fusami, O. Nweze, and R. Hassan, "Comparing the Effect of Deforestation Result by NDVI and SAVI," *International Journal of Scientific and Research Publications*, vol. 10, no. 6, pp. 918–925, Jun. 2020, <https://doi.org/10.29322/IJSRP.10.06.2020.p102110>.
- [27] "Saudi Arabia," *World Bank Climate Change Knowledge Portal*, <https://climateknowledgeportal.worldbank.org/country/saudi-arabia/climate-data-historical>.
- [28] G. Gutman and A. Ignatov, "The derivation of the green vegetation fraction from NOAA/AVHRR data for use in numerical weather prediction models," *International Journal of Remote Sensing*, vol. 19, no. 8, pp. 1533–1543, Jan. 1998, <https://doi.org/10.1080/014311698215333>.
- [29] S. Shastri, P. Singh, P. Verma, P. K. Rai, and A. P. Singh, "Land Cover Change Dynamics and their Impacts on Thermal Environment of Dadri Block, Gautam Budh Nagar, India," *Journal of Landscape Ecology*, vol. 13, no. 2, pp. 1–13, Sep. 2020, <https://doi.org/10.2478/jlecol-2020-0007>.
- [30] X. Gong, S. Du, F. Li, and Y. Ding, "Study of mesoscale NDVI prediction models in arid and semiarid regions of China under changing environments," *Ecological Indicators*, vol. 131, Nov. 2021, Art. no. 108198, <https://doi.org/10.1016/j.ecolind.2021.108198>.
- [31] J. Aryal, C. Sitaula, and S. Aryal, "NDVI Threshold-Based Urban Green Space Mapping from Sentinel-2A at the Local Governmental Area (LGA) Level of Victoria, Australia," *Land*, vol. 11, no. 3, Mar. 2022, Art. no. 351, <https://doi.org/10.3390/land11030351>.
- [32] I. Beveridge, "Mammal parasites in arid Australia," *International Journal for Parasitology: Parasites and Wildlife*, vol. 12, pp. 265–274, Aug. 2020, <https://doi.org/10.1016/j.ijppaw.2020.02.003>.